Life Sciences 237 (2019) 116978

Contents lists available at ScienceDirect

Life Sciences

journal homepage: www.elsevier.com/locate/lifescie

Ameliorative effects of echinacoside against spinal cord injury via inhibiting NLRP3 inflammasome signaling pathway

Shutao Gao, Tao Xu, Hailong Guo, Qiang Deng, Chuanhui Xun, Weidong Liang, Weibin Sheng*

Department of Spine Surgery, Xinjiang Medical University Affiliated First Hospital, Urumqi, Xinjiang, 830054, China

ARTICLE INFO

Keywords:
Echinacoside
NLRP3
Inflammasome
Microglia
Spinal cord injury

ABSTRACT

Aims: The activation of NLRP3 inflammasome, which initiates an inflammatory cascade and triggers inflammatory death, plays a crucial role in the pathogenesis of spinal cord injury (SCI). Echinacoside (ECH) is a phenylethanoid glycoside possessing prominent anti-inflammatory effects and various neuroprotective properties in the central nervous system, but the effect of ECH on SCI was rarely studied. Therefore, the purpose of this experiment was to look into the therapeutic effects of ECH on SCI and the underlying mechanisms.

Main methods: Basso-Beattie-Bresnahan (BBB) locomotion scale, Nissl staining, and hematoxylin-eosin (HE) staining was employed to examine the therapeutic effects of ECH on SCI. In addition, reactive oxygen species (ROS) generation, mitochondrial membrane potential (MMP) in BV-2 cells stimulated with lipopolysaccharides and adenosine 5′-triphosphate were examined. The expression levels of proteins involving NLRP3 inflammasome-related pathway were measured.

Key findings: The in vivo experiment indicated that administration of ECH significantly enhanced the BBB scores, reduced the neuron loss, and ameliorated the tissue architecture after SCI. Additionally, ECH dramatically inhibited NLRP3 inflammasome activation in the rat SCI model. In vitro study indicated that ECH significantly reduced ROS level, improved the MMP, blocked activation of NF-κB, and inhibited the NLRP3 inflammasome signaling pathway. The effect of ECH on inhibition of NLRP3 inflammasome signaling pathway was partially governed by suppression of the generation of ROS and activation of NF-κB.

Significance: ECH can accelerate motor function recovery in rats following SCI by inhibiting NLRP3 inflammasome-related signaling pathway, suggesting that ECH may serve as a potential therapeutic agent for treating SCI.

1. Introduction

Spinal cord injury (SCI), which is a condition mainly characterized by motor and sensory deficits below scathed segments, is a devastating event to affected individuals who usually experience a remarkable decrease in quality of life. Literature has reported that the prevalence of SCI ranges from 250 to 906 cases per million worldwide [1]. SCI has resulted in huge medical consumption and economic loss, and imposed a heavy burden on families and society. Despite enormous progress has been made in neuroscience and surgical treatment, SCI remains to be a major challenge in clinical work [2]. Thus, it is of great significance to investigate the underlying mechanism of SCI pathogenesis so as to develop an effective therapeutic strategy for this disease.

According to pathophysiological phases, SCI can be divided into primary injury and secondary injury [3]. As a result of intense physical forces of the traumatic event, primary SCI is irreversible. Correspondingly, secondary injury is a delayed and ongoing injury that leads to further functional loss, which can be blocked by appropriate treatment strategies. Concerning its reversibility, current treatments mainly focus on the secondary injury with an aim to provide a better microenvironment for resident cells in the spinal cord. Considerable evidences indicate that secondary injury of SCI is accompanied by diverse pathophysiologic mechanisms, including inflammatory response [4], endoplasmic reticulum stress [5,6], mitochondrial dysfunction [7,8], glutamate-induced excitotoxicity [9,10], as with excessive production of free radicals [11,12]. Of them, inflammatory response contributes greatly to the pathogenesis of SCI and makes it more difficult to restore [13,14]. How to effectively repress inflammatory response has become one of the focuses in SCI research.

In the past decade, a rapidly expanding literature demonstrates that inflammasomes play a crucial role during the inflammatory process after central nervous system injuries [15]. The inflammasomes are a

* Corresponding author. 137 Liyushan Avenue, Xinshi District, Urumqi, Xinjiang, 830054, China.
E-mail addresses: gaoshutoo@126.com (S. Gao), xt0005@sina.com (T. Xu), guohailong@tom.com (H. Guo), 1714250017@qq.com (Q. Deng), xunchuanhui@126.com (C. Xun), guxiaoliang06@sina.com (W. Liang), wbsheng@vip.sina.com (W. Sheng).

https://doi.org/10.1016/j.lfs.2019.116978
Received 17 September 2019; Received in revised form 7 October 2019; Accepted 15 October 2019
Available online 20 October 2019

cluster of cytosolic multi-protein complexes that function as receptors and sensors of immune system in response to exogenous and external damages through damage-associated molecular patterns (DAMPs) or pathogen-associated molecular patterns (PAMPs) [16]. NLRP3 inflammasome is the most widely studied inflammasome which participates in the transforming of inactive pro-caspase-1 to its active form. Once activated, caspase-1 proteolytically processes the pro-inflammatory cytokines of pro-interleukin (IL)-1β and pro-IL-18 into mature IL-1β and IL-18, which can drive a robust inflammatory cascade, eventually magnifying the inflammatory response. In the rodent SCI models, inhibition of the NLRP3 inflammasome exerted a prominently neuroprotective effect, demonstrating that NLRP3 inflammasome was a vital mediator during SCI [17]. Therefore, the NLRP3 inflammasome may be a novel target of pharmacological therapy for SCI.

Echinacoside (ECH) is a phenylethanoid glycoside isolated from Cistanches, which has been used as a herbal medicine for centuries in China [18]. Numerous studies have elucidated the beneficial properties of ECH, including anti-inflammatory, anti-oxidative, and anti-apoptosis activities [19]. Further studies also demonstrate that ECH exerts obviously neuroprotective effects [20–23].

However, thus far, no study has been carried out to look into whether ECH could influence NLRP3 inflammasome-driven inflammatory pathway after SCI. Hence, the main purpose of this study was to investigate the role of NLRP3 inflammasome in the therapeutic effects of ECH on SCI using an in vitro microglia injury model and an in vivo rat SCI model.

2. Materials and methods

2.1. Drugs and antibodies

ECH (HPLC ≥ 98.8%) was purchased from Must Bio-technology (Chengdu, China). Primary antibodies against NLRP3, caspase-1, p-NF-κB, and p-Iκ-Bα were purchased from Abcam (Massachusetts, USA). Primary antibodies against ASC, IL-18, IL-1β, NF-κB and Iκ-Bα were bought from Wuhan Proteintech Group (Wuhan, China). Primary antibody of NEK7 was obtained from Cell Signaling Technology (Beverly, Massachusetts, USA). Primary antibody of GAPDH was brought from Bioss (Beijing, China). Second antibodies for Western blot and immunofluorescence were provided by ZSJB-BIO (Beijing, China) and Elabscience Biotechnology (Wuhan, China), respectively. Information of antibodies was listed in Table 1. Adenosine 5′-triphosphate disodium salt (ATP) and lipopolysaccharide (LPS) were brought from Sigma-Aldrich (St Louis, MO, USA). All other chemicals and kits were commercially available.

2.2. Cell culture and treatment

BV-2 cells are a murine cell line, which is generated by transfecting v-raf/v-myc oncogene into primary microglial cells of one-week old C57BL/6 mice [24]. They are immortalized cells and widely used as substitute for primary microglia. BV-2 cell line was obtained from cell bank of Wuhan University (Wuhan, China). Briefly, BV-2 cells were cultured in RPMI-1640 medium supplemented with 10% fetal bovine serum (Gibco, Australia), 100 U/mL penicillin and 100 μg/mL streptomycin (HyClone, USA) at 37 °C with 5% CO2 in a humidified cell incubator. To induce the activation of NLRP3 inflammasome, BV-2 cells were stimulated with 500 ng/ml LPS for 12 h, followed by 1 mM ATP for 30 min.

2.3. Cell viability assays

Cell Counting Kit-8 (CCK-8) assays were used to estimate the cytotoxic effect of ECH. In brief, BV-2 cells were seeded into 96-well plates (1×10^4 cells/well) with 100 μl RPMI-1640 medium per well in the presence of ECH at gradient concentrations (1, 2, 5, 10, 20, 50, 100, and 200 μg/ml) for 24 h and 48 h, BV-2 cells without ECH were designed as the control group. At the end of the stimulation time, 10 μl CCK-8 solution was added into each well, incubated at 37 °C for 1 h. Finally, absorbance of each well was measured at 450 nm by a Microplate reader (Thermo, USA).

2.4. Measurement of reactive oxygen species

Intracellular reactive oxygen species (ROS) was measured by flow cytometry using ROS assay kits (Beyotime Biotechnology, Jiangsu, China). BV-2 cells were seeded into 6-well plates (2×10^6 cells/well) and routinely cultured. When the confluence reached 70%, BV-2 cells were administrated with 500 ng/ml LPS for 12 h followed by 1 mM ATP for 0.5 h, in the presence of ECH (0, 10, 20, or 50 μg/ml). BV-2 cells without any stimulation were considered as control group. At the end of ECH treatment, BV-2 cells were washed twice with basic RPMI-1640 medium and loaded with 10 μM dichlorofluorescin diacetate (DCFH-DA), incubated at 37 °C for 30 min. After that, the cells were trypsinized for the detection of ROS by the flow cytometer (BD Biosciences, USA).

2.5. Detection of mitochondrial membrane potential

The mitochondrial membrane potential (MMP) was examined by using Mito-Tracker Red probe (Beyotime, China). BV-2 cells given different treatments as above described were incubated at 37 °C with RPMI-1640 medium supplemented with 20 nM Mito-Tracker Red for 30 min. Nuclei were stained by DAPI (Boster, Wuhan, China) and

Table 1
Main information of primary and secondary antibodies.

Antibody	Supplier	Catalog#	Source	Dilution	
				WB	IF
GAPDH	Bioss	bs-2188R	Rabbit	1: 20000	—
NLRP3	Abcam	ab214185	Rabbit	1: 1000	1: 300
ASC	Wuhan Proteintech Group	10500-1-AP	Rabbit	1: 1000	—
Caspase-1	Abcam	ab1872	Rabbit	1: 1000	—
NEK7	Cell Signaling Technology	#3057	Rabbit	1: 1000	—
IL-18	Wuhan Proteintech Group	10663-1-AP	Rabbit	1: 1000	—
IL-1β	Wuhan Proteintech Group	10806-1-AP	Rabbit	1: 1000	—
NF-κB	Wuhan Proteintech Group	10745-1-AP	Rabbit	1: 2500	—
p-NF-κB	Abcam	ab86299	Rabbit	1: 2500	—
Iκ-Bα	Wuhan Proteintech Group	10268-1-AP	Rabbit	1: 2500	—
p- Iκ-Bα	Abcam	ab133462	Rabbit	1: 2500	—
Peroxidase-conjugated second antibody	ZSGB-Bio	ZB-2301	Goat	1: 25000	—
FITC-conjugated second antibody	Elabscience	E-AB-1014	Goat	—	1: 100

photographed with a confocal microscope (Olympus Inc., Japan). Fluorescence intensity was quantified through Image J software.

2.6. Immunofluorescence staining

BV-2 cells were seeded into 24-well plates with glass coverslips (2×10^5 cells/well). When the confluence reached 50%, BV-2 cells were stimulated as abovementioned. After fixation with 4% paraformaldehyde (PFA), BV-2 cells were permeabilized with Triton X-100 for 15 min, blocked with 5% bovine serum albumin (Sigma, USA) for 60 min, and incubated with primary NLRP3 antibody overnight. Then, the cells were incubated with FITC-conjugated second antibody for 1 h and labeled with DAPI for 10 min. Finally, coverslips were observed in a confocal fluorescence microscope (Olympus Inc., Japan).

2.7. Animals, experimental design, and surgical procedure

Adult male Sprague-Dawley (SD) rats (180–220 g) were bought from the Animal Center of Xinjiang Medical University. The rats were kept with free access to water and food for seven days to adapt to the environment before experiments, on a 12 h light/dark cycle, under standard temperature- and humidity-controlled conditions. All animal protocols were approved by the Ethics Committee of Xinjiang Medical University Affiliated First Hospital (IACUC-20190225-11).

The rats were randomly assigned into three groups: (i) sham group, rats were subjected to T9 laminectomy and administered with daily 0.5 ml 0.9% sodium chloride by intraperitoneal injection; (ii) SCI group, rats were subjected to T9 SCI and administered with daily 0.5 ml 0.9% sodium chloride by intraperitoneal injection; (iii) SCI + ECH, rats were subjected to T9 SCI and administered with daily ECH (20 mg/kg) dissolved in 0.5 ml 0.9% sodium chloride by intraperitoneal injection.

SCI was induced by the Allen's method. Briefly, rats were anesthetized with intraperitoneal injection of 30 mg/kg pentobarbital sodium. Laminectomy was carried out to expose the spinal cord at vertebral T9 to T11 segments. The spinal cord at vertebral T10 segment received a 10 g impactor dropped by a 25 mm height. After that, rats were administered intramuscular injections of penicillin (40×10^5 unit/animal/day) and buprenorphine (0.01 mg/kg) to prevent infection and relieve pain. In addition, the rats received manual bladder emptying twice a day.

2.8. Neurological scoring

The neurological deficit of each rat was assessed by using Basso, Beattie, and Bresnahan (BBB) locomotor test [25]. Assessment was carried out before surgery and at 1st, 3rd, 7th, 14th, 21st, 28th, and 35th day post-surgery by two independent investigators who were blinded to the experimental conditions.

2.9. Tissue preparation

For Western blot experiment, the spinal cords were removed directly after euthanasia at the 3rd day following surgery. For staining experiment, the rats were perfused with 0.9% sodium chloride followed by 4% PFA at 7th day after surgery. The spinal cord tissues were resected with the epicenter included, and immersed in 4% PFA. The immersion liquid was replaced with 30% sucrose solution 24 h later. Then, 10 μm crosswise sections were prepared for Nissl straining and hematoxylin-eosin (HE) staining.

2.10. Nissl straining and hematoxylin-eosin staining

To evaluate neuronal survival and morphological changes of spinal cord, Nissl staining and HE staining were performed respectively. For Nissl straining, sections were dewaxed with xylene, rehydrated in graded concentrations of ethanol, treated with Nissl staining solution (Boster, China). Only cells with visible nuclei and typical neuronal morphology were counted. For each rat, every other continuous section was selected and a total of three sections were counted. The ventral motor neurons were counted for the quantitative statistics analysis by Image J software [26]. For HE straining, sections were stained with hematoxylin followed by eosin, and permeabilized with xylene.

2.11. Protein extraction and Western blot

Spinal cord tissues were dissected 5 mm above and below the injury site, homogenized using RIPA buffer containing phosphatase and protease inhibitors (Solarbio, Beijing, China). The supernatant was collected after centrifugation at 12000*g*, 4 °C for 30 min. For cultured BV-2 cells, they were lysed with RIPA buffer on ice for 30 min, the following steps were similar to the protein extraction of BV-2 cells. Protein concentration was measured with a BCA Protein Assay Kit (Solarbio, China). SDS-PAGE loading buffer (Solarbio, China) was added to the supernatant, and heated at 100 °C for 5 min. Protein samples (30 μg) were loaded and electrophoresed on 10% SDS-polyacrylamide gels, transferred to a 0.22 μm polyvinylidene difluoride membrane (Roche, Mannheim, Germany), blocked with 5% skim milk (for phosphorylated target proteins, bovine serum albumin was used), and incubated with primary antibodies overnight at 4 °C. Then, the membranes were incubated with rabbit HRP-conjugated secondary antibody at room temperature for 1 h. Protein band signals were visualized by ECL chemiluminescence substrate (Thermo, USA). Image J software was used for data analysis, and band intensity was normalized to that of GAPDH.

2.12. Statistical analysis

SPSS statistics version 22 was used for statistical analyses. The results were presented as mean ± standard deviation (SD). Two groups with normal distribution were analyzed using unpaired Student's t test. One-way ANOVA with LSD post hoc analysis were employed for multiple comparisons to assess differences among all groups. Differences were considered to be statistically significant when $P < 0.05$.

3. Results

3.1. ECH had no cytotoxic effect on BV-2 cells

The chemical structure of ECH was displayed in Fig. 1A. CCK-8 assays were applied to investigate the effect of ECH on the viability of BV-2 cells. As demonstrated in Fig. 1B-C, the results indicated that administration of ≤100 μg/ml ECH at 24 and 72 h had no significant cytotoxic effect on BV-2 cells. Therefore, 10, 20, and 50 μg/ml ECH were selected for further experiments, as precious literature has reported [27].

3.2. ECH promoted motor function recovery, alleviated structural disorder and neuron loss following SCI

BBB scores of rats in both SCI group and SCI + ECH group gradually increased with time elapsed, but the ECH treatment group scored better than the SCI group, especially from the 3rd day after operation ($P < 0.05$, Fig. 2A). These data indicated that ECH could effectively advance the recovery of hindlimb motor function following SCI. The Nissl staining and HE staining were employed to evaluate the morphological changes of spinal cords. Worse texture disorder and abnormal tissue arrangement were witnessed in the SCI group, whereas ECH significantly ameliorated the histological morphology (Fig. 2B). For Nissl staining, the number of survival neurons was quantitated by counting of intact neurons located in the ventral horn, and fewer neurons were lost in the SCI + ECH group than that in the SCI group ($P < 0.01$, Fig. 2C-D). The above data suggested that ECH reduced tissue disorder and neuron loss, and improved the motor function after

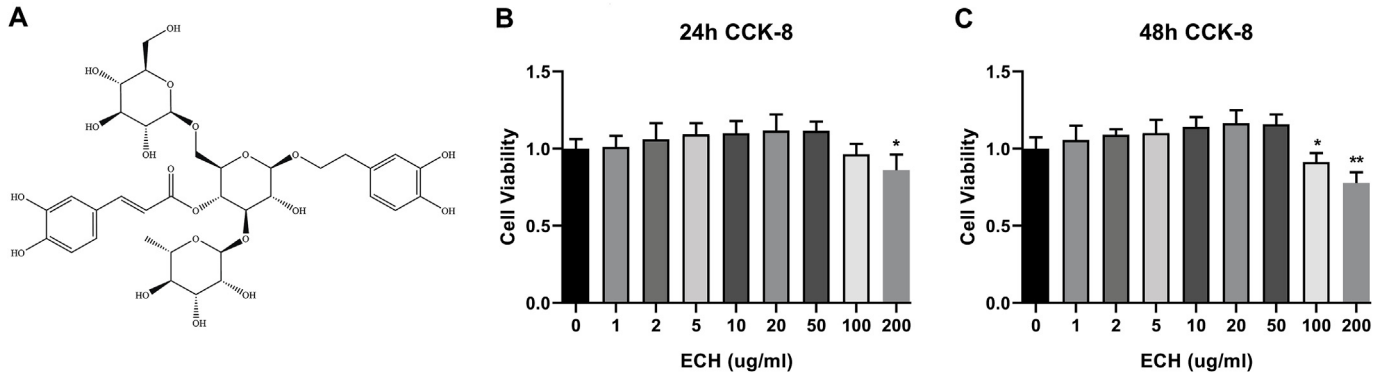

Fig. 1. Effects of ECH on the viability of BV-2 cells. A, The chemical structure of ECH; B–C, The cytotoxic effect of ECH on BV-2 cells was examined at different concentrations for 24 h and 48 h by using CCK-8 assays. There was a significant reduction in cell viability treated with ECH at the concentration of ≥100 μg/ml. The values presented were the mean ± SD of three independent experiments. $^{*}P < 0.05$, $^{**}P < 0.01$.

SCI.

3.3. ECH inhibited the NLPR3 inflammasome signal pathway in LPS/ATP induced BV-2 cells and SCI rats

To investigate whether ECH suppressed the activation of NLRP3 inflammasome, the expressions of NLPR3 inflammasome-related proteins were detected in LPS/ATP-induced BV-2 cells in present or absent of ECH. The stimulation of LPS/ATP significantly increased the expression of NLPR3 inflammasome-associated proteins, including NEK7, NLRP3, ASC, caspase-1, IL-18, and IL-1β ($P < 0.01$, Fig. 3A-G). Whereas, administration of ECH prominently inhibited these protein expressions in a dose-dependent manner ($P < 0.05$, Fig. 3A-G). Additionally, concerning NLRP3 was the core protein in the NLRP3 inflammasome signaling pathway, we investigated the expression of the NLRP3 through immunofluorescence. Similarly, BV-2 cells treated with ECH resulted in reduced fluorescent intensity in a concentration-dependent manner, suggesting ECH obviously down-regulated the expression of NLRP3 (Fig. 3H). In agreement with the findings of in vivo experiment, SCI-induced increase of NLRP3 inflammasome-related proteins were also significantly decreased by the administration of ECH (Fig. 4A-G). The data of both in vivo and in vitro experiments suggested that ECH inhibited the NLRP3 inflammasome signal pathway in LPS/ATP treated BV2 cells and SCI model of rat.

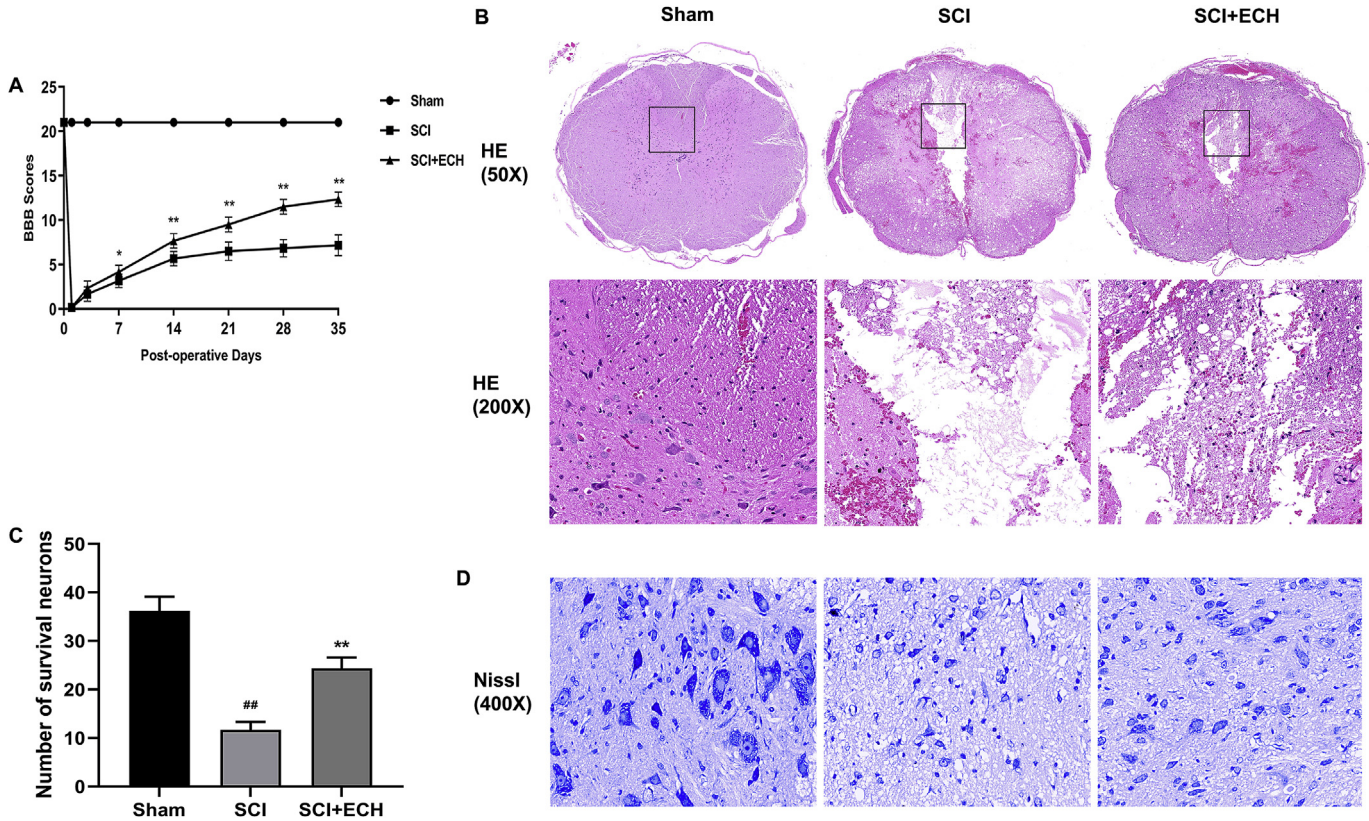

Fig. 2. ECH improved functional recovery of hindlimb motor and ameliorated structural disorder with less neuron loss following SCI. A, The BBB scores at 0, 1, 7, 14, 21, 28, and 35 days of each group. B, Representative images of HE staining at 7th day after surgery. C, the number of surviving neurons was counted after Nissl staining at 7th day following surgery. D, Representative Nissl staining of spinal motor neurons at 7th day after SCI. $^{*}P < 0.05$, $^{**}P < 0.01$, compared with SCI group; $^{\#\#}P < 0.01$, Compared with the sham group; n = 6 per group. All data were presented as mean ± SD. SCI, spinal cord injury; BBB scores, The Basso, Beattie and Bresnahan scores; HE, Hematoxylin-Eosin.

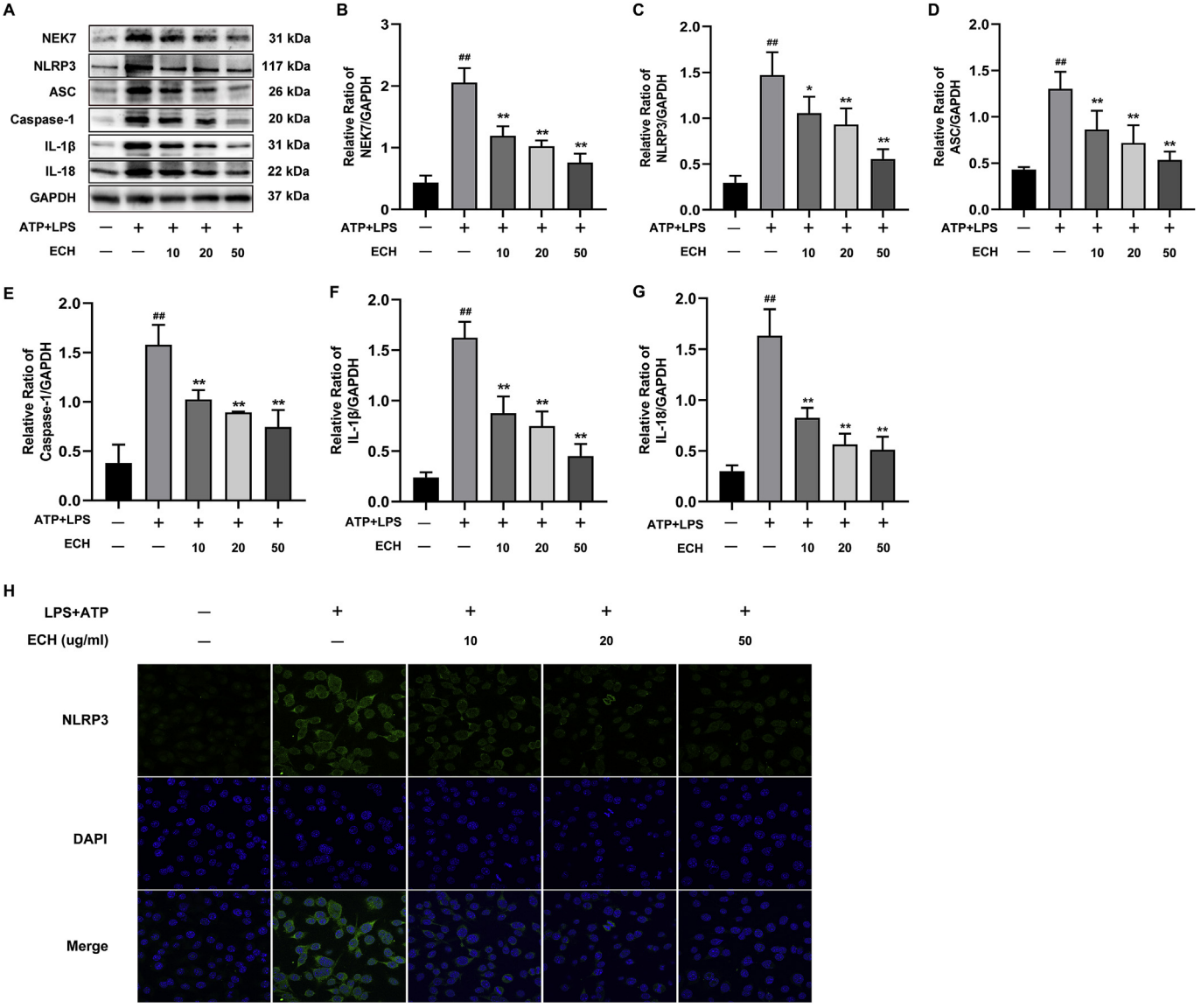

Fig. 3. ECH inhibited NLRP3 inflammasome signaling pathway in LPS/ATP-induced BV-2 cells. BV-2 cells were treated with 500 ng/ml LPS for 12 h followed by 1 mM ATP for 0.5 h, in or without the presence of ECH (0, 10, 20, or 50 μg/ml). BV-2 cells without any stimulation were considered as control group. Protein expression was detected by Western blot and immunofluorescence straining. A, The expressions of NEK7, NLRP3, caspase-1, ASC, IL-1β, and IL-18 in BV-2 cells; B-G, The relative intensity of each band was quantitated in NEK7 (B), NLRP3 (C), caspase-1 (D), ASC (E), IL-1β (F), and IL-18 (G), GAPDH was utilized as a loading control; H, Immunofluorescence images of NLRP3 (magnification, 600 X); I, Quantitative analysis of NLRP3 fluorescent intensity. All results were representative of three independent experiments. The data were presented as mean ± SD. $^{\#}P < 0.05$, $^{\#\#}P < 0.01$ compared with control group, $^{*}P < 0.05$, $^{**}P < 0.01$ compared with LPS/ATP group.

3.4. ECH inhibited LPS/ATP-induced NF-κB pathway in BV-2 cells

Emerging evidences have demonstrated that NF-κB pathway plays a crucial role in mediating the inflammatory response. To further analyze the anti-inflammatory mechanism of ECH, Western blot was employed to detect whether ECH could inhibit the expression of NF-κB pathway-related proteins in BV-2 cells upon LPS/ATP stimulation. Notably, stimulation with LPS/ATP enhanced the levels of p-NF-κB (p-p65) and p-Iκ-Bα proteins when compared with that in the control, whereas administration of ECH strikingly reversed the ratios of p-p65 and p-Iκ-Bα in a concentration-dependent manner (Fig. 5A-C, $P < 0.01$). Collectively, these findings suggested that ECH remarkably impeded LPS/ATP -induced activation of NF-κB pathway in BV-2 cells.

3.5. ECH prevented LPS/ATP induced mitochondrial dysfunction in BV-2 cells

MitoTracker Red is a red fluorescent dye dependent on MMP in mitochondria. As displayed in Fig. 6A-B, stimulation with LPS/ATP resulted in significantly decreased intensity of red fluorescence. However, administration of ECH rescued the loss of fluorescence intensity ($P < 0.01$). These data indicated that ECH could protect mitochondria from damage.

3.6. Echinacoside inhibited the production of ROS in BV-2 cells

To investigate whether ECH had an effect on the production of ROS in BV-2 cells, we measured intracellular ROS production through flow cytometry. Obtained data showed that upon exposure to LPS/ATP, the intracellular ROS production significantly increased, indicating LPS/

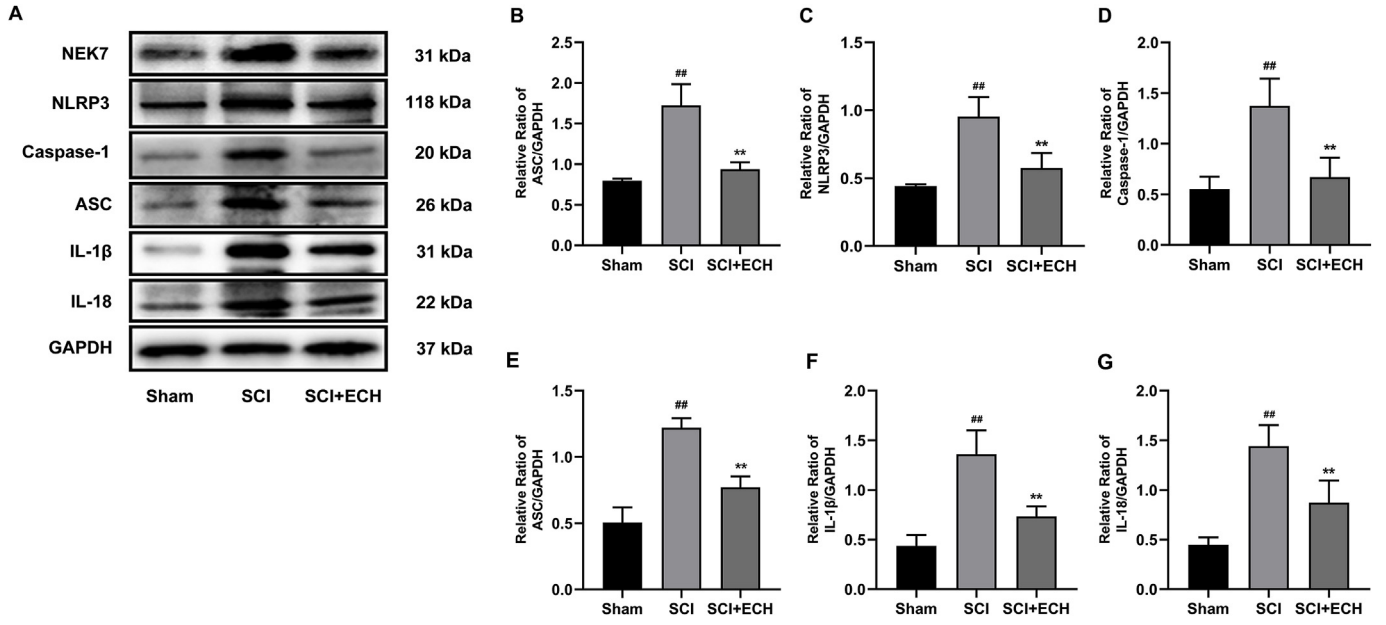

Fig. 4. ECH inhibited NLRP3 signaling pathway in spinal cord injury model of rats. A, The protein expressions of NEK7, NLRP3, caspase-1, ASC, IL-1β, and IL-18 in spinal cord tissue were detected by Western blot at 3rd day following SCI. B-G, The relative intensity of each band was quantitated in NEK7 (B), NLRP3 (C), caspase-1 (D), ASC (E), IL-1β (F), and IL-18 (G). GAPDH was employed as a loading control. Above results were obtained from three independent experiments, each group consisted of 6 rats. The data were presented as mean ± SD. $^{\#\#}P < 0.01$ compared with sham group, $^{**}P < 0.01$ compared with SCI group.

ATP enhanced the generation of ROS in BV-2 cells. However, treatment with ECH was able to effectively reduce the ROS generation (Fig. 6C-D, $P < 0.01$).

4. Discussion

Traumatic strike to spinal cord elicits an intense inflammatory response including rapid activation of microglia and release of pro-inflammatory cytokines, which subsequently enlarge the vulnerable perilesional region and induce permanent damage [28]. Given the pivotal nature of inflammatory changes after SCI, blockage of the inflammatory context is an extremely important area of translational research and may provide a desirable therapeutic strategy to reduce tissue damage and promote recovery.

As a natural extract of plants, ECH had displayed its excellent anti-inflammatory and neuroprotective effects. Precious studies have demonstrated that ECH has beneficial effects on CNS disorders like ischemic brain injury [20], Alzheimer's disease [29], and Parkinson's disease [22]. However, the effect of ECH on SCI has not been investigated thus far. In the early stage of this experiment, the safe concentration of ECH on BV-2 cells was determined by CCK-8 arrays. Three different concentrations containing 10, 20, and 50 μg/ml were applied in the following study. For the in vivo study, the most commonly used dose of 30 mg/kg was employed [18]. The findings of our in vivo experiment highlighted that ECH ameliorated motor function of lower limbs as with reduced tissue damage of SCI in rats. In addition, it was witnessed that ECH inhibited the activation of NLRP3 inflammasome both in vivo and in vitro. These findings indicated that ECH played a neuroprotective effect through its NLRP3 inflammasome-associated anti-inflammatory property, suggesting the potentially therapeutic effect of ECH on SCI. The findings of this study also broadened the understanding of anti-inflammatory and neuroprotective mechanism of ECH on SCI.

The essential components of NLRP3 inflammasome, which include NLRP3, caspase-1, as with ASC, always exist separately in the cytoplasm. Upon stimulates, these components aggregate to form into NLRP3 inflammasome. Excessive NLRP3 inflammasome formation promotes sustained inflammatory response that gives rise to the development of various diseases. The role of NLRP3 inflammasome in the progression of SCI has gained a growing attention and extensive studies have linked it to the secondary damage phase of SCI [30]. Therefore, interventions to suppress the activation of NLRP3 inflammasome may

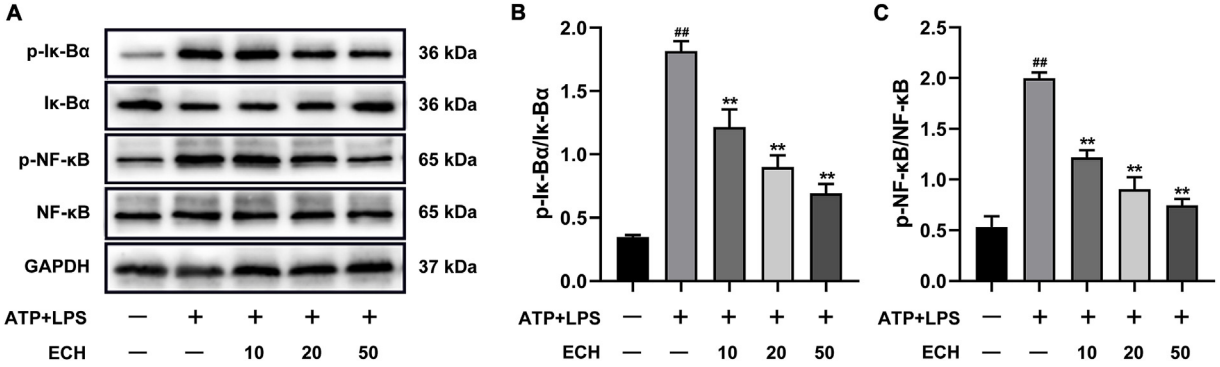

Fig. 5. ECH inhibited NF-κB signaling pathway in LPS/ATP-induced BV-2 cells. A, Representative western blots of p-NF-κB, NF-κB, p-Iκ-Bα, and Iκ-Bα; B, Quantitative analysis of p-Iκ-Bα/Iκ-Bα; C, Quantitative analysis of p-NF-κB/NF-κB. GAPDH was utilized as a loading control. All results were representative of three independent experiments. The data were presented as mean ± SD. $^{\#\#}P < 0.01$ compared with control group, $^{**}P < 0.01$ compared with LPS/ATP group.

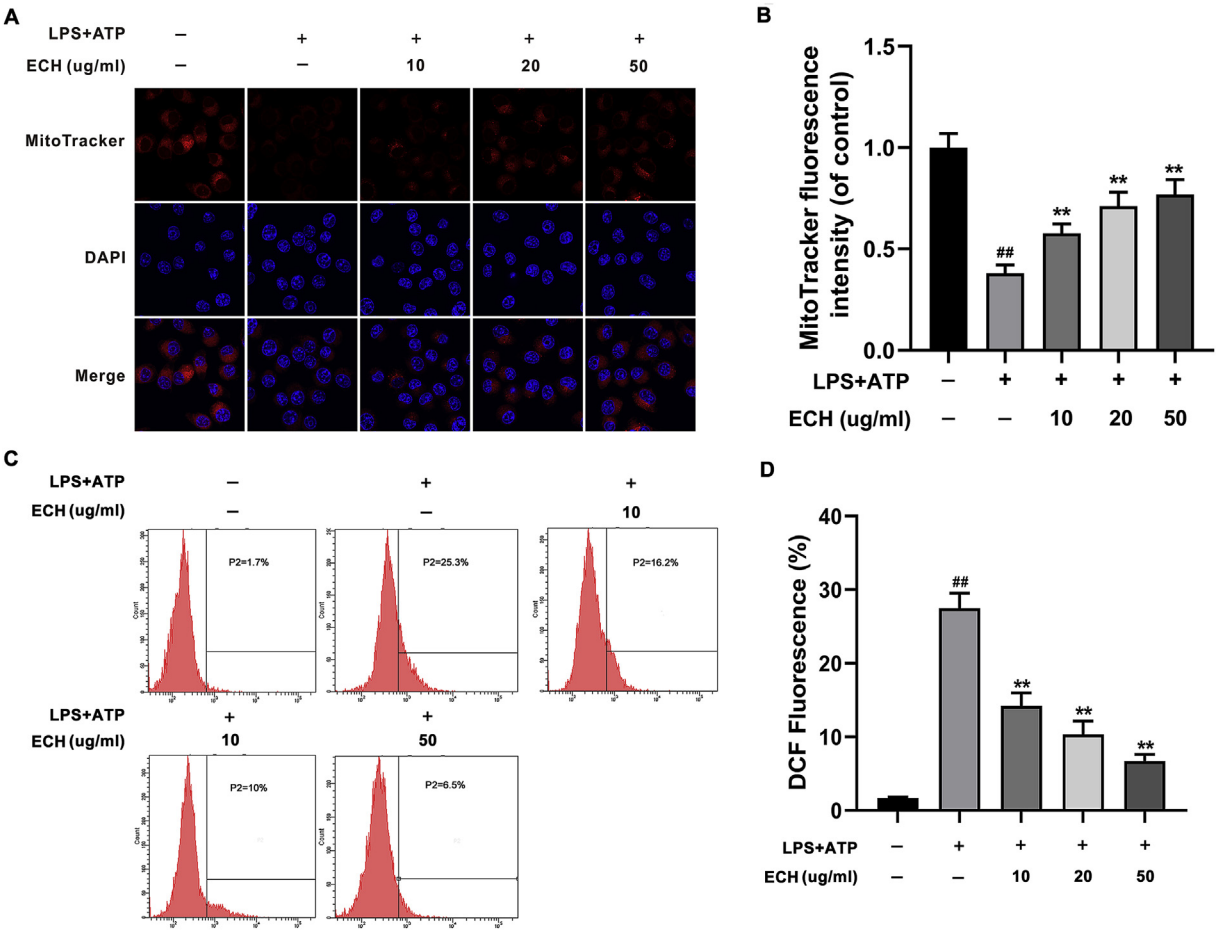

Fig. 6. ECH alleviated mitochondrial dysfunction and inhibited the generation of ROS in LPS/ATP-induced BV-2 cells. A, Mitotracker assay showed that stimulation with LPS/ATP remarkably decreased the membrane potential, administration of ECH reversed this effect (magnification, 1200X); B, The quantification of mitotracker fluorescence intensity of each group. C, Measurement of cellular ROS by flow cytometry; D, Quantification of ROS production, the bar graph represented DCF fluorescence intensity of the each group. The values presented were the mean ± SD of three independent experiments. $^{\#\#}P < 0.01$ compared with control group, $^{**}P < 0.01$ compared with LPS/ATP group.

serve as a novel approach to ameliorate outcomes following SCI. Activation of NLRP3 inflammasome always involves two distinct steps, which are known as priming (signal 1) and activation (signal 2) [31]. The priming step initiates the NF-κB-mediated up-regulation of NLRP3, pro-IL-18, and pro-IL-1β for efficient inflammasome formation. This step is followed by activation step which can be triggered by DAMPs, resulting in the oligomerization and assembly of the NLRP3 inflammasome (Fig. 7) [32]. Our findings also demonstrated the NLRP3 inflammasome might be a potential target for pharmacological inhibition following SCI, as NLRP3, caspase-1, IL-1β, and IL-18 were significantly enhanced after SCI and ECH obviously suppressed the expression of those NLRP3 inflammasome-related proteins.

NF-κB is a ubiquitous inducible transcription factor that governs the expression of most genes and regulates a range of cellular functions. It has been considered as a critical contributor and a robust regulator in the transcription of pro-inflammatory mediators and cytokines [33]. Literature has shown that NF-κB could induce the expression of NLRP3 infalmmasome-related genes, and the latter are further required for the formation of NLRP3 inflammasome complexes [34]. Therefore, we looked into whether ECH could inhibit the activation of NLRP3 inflammasome through down-regulating NF-κB signaling pathway. Phosphorylation of NF-κB and IκBα are required for the initiation of NF-κB signaling pathway. Data obtained from our in vitro experiment indicated that the protein levels of phosphorylated NF-κB (p-p65) and IκBα (p-IκBα) were significantly up-regulated with the stimulation of LPS/ATP in BV-2 cells, and administration of ECH reversed the levels of p-p65 and p-IκBα, indicating ECH acted as a negative regulator in the NF-κB signal pathway during NLRP3 inflammasome activation. Actually, precious studies had revealed that ECH had an effect on NF-κB signal pathway. Kuang et al. [35] reported that ECH down-regulated NF-κB p-65 in H_2O_2-induced PC12 cells, thus protecting PC12 cells against damage. Zhang et al. [36] demonstrated that ECH exerted neuroprotective efects through down-regulating the NF-κB p-52 signaling pathway. The above evidence supported that ECH could inhibited the NF-κB signal pathway, and our experiment further demonstrated that ECH could suppressed the activation of NLRP3 infmammasome through downregulating NF-κB p-65 pathway.

Mitochondrial dynamics exert a crucial physiological role in maintaining cell homeostasis [37]. ROS, which is mainly produced by mitochondria, has been proposed to be a pivotal regulator of inflammatory response and a major trigger for the activation of NLRP3 inflammasome [31,38]. The generation of mitochondrial ROS could be induced by NLRP3 inflammasome agonists, and inhibition of ROS abrogated the activation of NLRP3 inflammasome [39]. Zhou et al. [40] reported that NLRP3 inflammasome could sense mitochondrial dysfunction. Once mitochondrial activity was inhibited, ROS generation and inflammasome activation were also suppressed [40]. Previous evidences have indicated that ROS is implicated in the development of secondary SCI, and suppression of ROS is of great importance to the survival of neural cells and the treatment of SCI [41]. As a product of cellular energy metabolism, overproduction of ROS may contribute to the mitochondrial dysfunction. Conversely, damaged mitochondria,

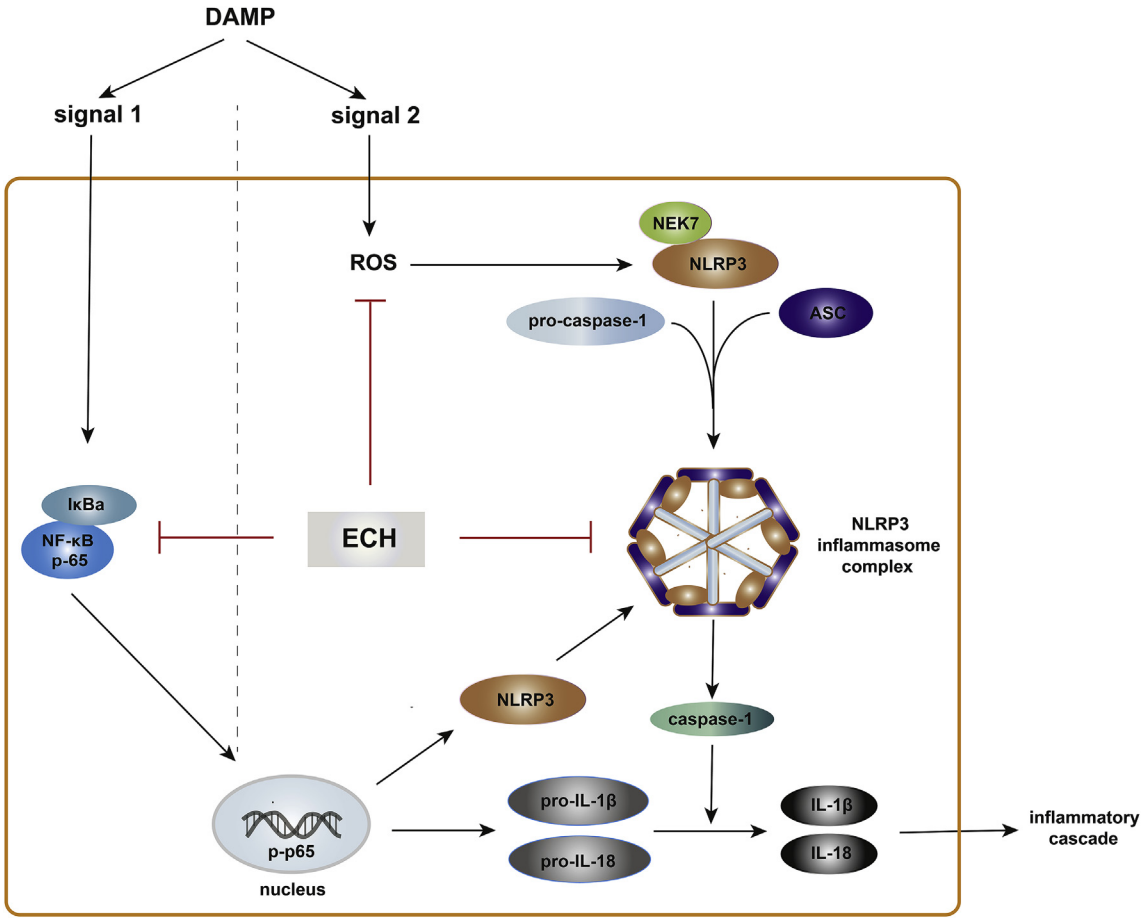

Fig. 7. Diagram of the putative mechanisms by which ECH inhibited the activation of NLRP3 inflammasome in BV-2 cells.

which are characterized with lower MMP, generate much more ROS and give rise to the release of molecules like mitochondrial DNA and mitochondrial ROS, thus leading to the NLRP3 inflammasome activation [39]. As a matter of fact, precious evidences have supported the beneficial effect of ECH in the down-regulation of ROS. ECH treatment has been shown to significantly attenuate the production of ROS and ameliorate the mitochondrial dysfunction in damaged PC12 cells [42]. Zhao et al. also reported that ECH significantly improved SH-SY5Y cells survival by inhibiting the generation of ROS induced by 1-methyl-4-phenylpyridinium ion [27]. Parallel to those precious evidences, our data indicated that ECH alleviated the intracellular accumulation of ROS, improved the MMP in LPS/ATP-stimulated BV-2 cells. The suppressive effect of ECH on NLRP3 inflammasome might partly attribute to the inhibition of ROS generation.

Recent publications have reported that NEK7 promoted the NLRP3-dependent inflammatory response, as it was also required for the oligomerization and activation of NLRP3 inflammasome by binding to NLRP3 leucine-rich repeat domain, which was in the downstream of mitochondrial ROS [43,44]. The maturation of caspase-1 and release of IL-1β appeared to be abrogated in the NEK7-deficient macrophages [44]. Another study reported that the formation NLRP3-dependent pyroptosome was dampened in macrophages that were in the absence of NEK7, indicating that NEK7 might functioned specifically upstream of NLRP3 inflammasome [45]. The present study found that the expression of NEK7 significantly elevated after SCI and stimulation with LPS/ATP in BV-2 cells, and the administration of ECH could remarkably reversed the elevation of NEK7. Nevertheless, whether ECH regulated the interaction of NEK7 and NLRP3 remains to be clarified. And further studies are still required to gain insight into the underlying mechanisms.

Several limitations existed in this study should be overcome in future work. First, BV-2 cell line was selected as an alternative for primary spinal cord microglia. Nevertheless, it is noteworthy that BV-2 cell is not an ideal substitute for microglia as literature has found several differences between them. Hence, further investigation in primary microglia is greatly encouraged [46]. Second, we only examined the short-term (less than 5 weeks) effect of ECH on SCI rats, long-term (more than 5 weeks) observations are still warranted. Third, as for administration dose of ECH in animal study, we selected 30 mg/kg/d as most previous literatures have reported [18]. It remains to be determined whether the therapeutic effect of ECH on SCI rats has a dose-dependence. Fourth, during the in vitro study, we did not investigated the effect of ECH on other spinal cord resident cells like neuron, astrocyte and oligodendrocyte, which are also reported to participant in the NLRP3 inflammasome signaling pathway [16,47].

5. Conclusion

The present study suggests that ECH is able to attenuate neuroinflammation by inhibiting NLRP3 inflammasome activation, consequently improves neurological function following SCI (Fig. 7). The findings indicate that ECH may serve as a promising therapeutic agent for SCI.

Declaration of competing interestCOI

The authors declare that there are no conflicts of interest.

Acknowledgement

None.

References

[1] A. Singh, L. Tetreault, S. Kalsi-Ryan, A. Nouri, M.G. Fehlings, Global prevalence and incidence of traumatic spinal cord injury, Clin. Epidemiol. 6 (2014) 309–331.
[2] J.H. Badhiwala, C.S. Ahuja, M.G. Fehlings, Time is spine: a review of translational advances in spinal cord injury, J. Neurosurg. Spine 30 (1) (2018) 1–18.
[3] S. Nori, C.S. Ahuja, M.G. Fehlings, Translational advances in the management of acute spinal cord injury: what is new? what is hot? Neurosurgery 64 (CN_suppl_1) (2017) 119–128.
[4] G. Khayrullina, S. Bermudez, K.R. Byrnes, Inhibition of NOX2 reduces locomotor impairment, inflammation, and oxidative stress after spinal cord injury, J. Neuroinflammation 12 (2015) 172.
[5] S. Liu, C. Sarkar, M. Dinizo, A.I. Faden, E.Y. Koh, M.M. Lipinski, J. Wu, Disrupted autophagy after spinal cord injury is associated with ER stress and neuronal cell death, Cell Death Dis. 6 (2015) e1582.
[6] Q. Wang, H. Cai, Z. Hu, Y. Wu, X. Guo, J. Li, H. Wang, Y. Liu, Y. Liu, L. Xie, K. Xu, H. Xu, H. He, H. Zhang, J. Xiao, Loureirin B promotes axon regeneration by inhibiting endoplasmic reticulum stress: induced mitochondrial dysfunction and regulating the Akt/GSK-3beta pathway after spinal cord injury, J. Neurotrauma 36 (2019) 1949–1964.
[7] N.E. Scholpa, R.G. Schnellmann, Mitochondrial-based therapeutics for the treatment of spinal cord injury: mitochondrial biogenesis as a potential pharmacological target, J. Pharmacol. Exp. Ther. 363 (3) (2017) 303–313.
[8] G. Li, Z. Jia, Y. Cao, Y. Wang, H. Li, Z. Zhang, J. Bi, G. Lv, Z. Fan, Mitochondrial division inhibitor 1 ameliorates mitochondrial injury, apoptosis, and motor dysfunction after acute spinal cord injury in rats, Neurochem. Res. 40 (7) (2015) 1379–1392.
[9] E. Park, A.A. Velumian, M.G. Fehlings, The role of excitotoxicity in secondary mechanisms of spinal cord injury: a review with an emphasis on the implications for white matter degeneration, J. Neurotrauma 21 (6) (2004) 754–774.
[10] D. Liu, J. Chen, T. Jiang, W. Li, Y. Huang, X. Lu, Z. Liu, W. Zhang, Z. Zhou, Q. Ding, H.A. Santos, G. Yin, J. Fan, Biodegradable spheres protect traumatically injured spinal cord by alleviating the glutamate-induced excitotoxicity, Adv. Mater. 30 (14) (2018) e1706032.
[11] C. Rios, I. Santander, M. Mendez-Armenta, C. Nava-Ruiz, S. Orozco-Suarez, M. Islas, V. Baron-Flores, A. Diaz-Ruiz, Metallothionein-I + II reduces oxidative damage and apoptosis after traumatic spinal cord injury in rats, Oxid. Med. Cell. Longev. (2018) 3265918(2018), PMID: 30524652.
[12] H. Ishii, A.B. Petrenko, M. Sasaki, Y. Satoh, Y. Kamiya, T. Tobita, K. Furutani, M. Matsuhashi, T. Kohno, H. Baba, Free radical scavenger edaravone produces robust neuroprotection in a rat model of spinal cord injury, Brain Res. 1682 (2018) 24–35.
[13] R. Putatunda, J.R. Bethea, W.H. Hu, Potential immunotherapies for traumatic brain and spinal cord injury, Chin. J. Traumatol. 21 (3) (2018) 125–136.
[14] M.B. Orr, J.C. Gensel, Spinal cord injury scarring and inflammation: therapies targeting glial and inflammatory responses, Neurotherapeutics 15 (3) (2018) 541–553.
[15] J.P. de Rivero Vaccari, W.D. Dietrich, R.W. Keane, Therapeutics targeting the inflammasome after central nervous system injury, Transl. Res. 167 (1) (2016) 35–45.
[16] M.K. Mamik, C. Power, Inflammasomes in neurological diseases: emerging pathogenic and therapeutic concepts, Brain 140 (9) (2017) 2273–2285.
[17] K. Mortezaee, N. Khanlarkhani, C. Beyer, A. Zendedel, Inflammasome: its role in traumatic brain and spinal cord injury, J. Cell. Physiol. 233 (7) (2018) 5160–5169.
[18] J. Liu, L. Yang, Y. Dong, B. Zhang, X. Ma, Echinacoside, an inestimable natural product in treatment of neurological and other disorders, Molecules 23 (5) (2018).
[19] Z. Fu, X. Fan, X. Wang, X. Gao, Cistanches Herba, An overview of its chemistry, pharmacology, and pharmacokinetics property, J. Ethnopharmacol. 219 (2018) 233–247.
[20] W. Wei, X.B. Lan, N. Liu, J.M. Yang, J. Du, L. Ma, W.J. Zhang, J.G. Niu, T. Sun, J.Q. Yu, Echinacoside alleviates hypoxic-ischemic brain injury in neonatal rat by enhancing antioxidant capacity and inhibiting apoptosis, Neurochem. Res. 44 (7) (2019) 1582–1592.
[21] H. Ma, Y. Liu, L. Tang, H. Ding, X. Bao, F. Song, M. Zhu, W. Li, Echinacoside selectively rescues complex I inhibition-induced mitochondrial respiratory impairment via enhancing complex II activity, Neurochem. Int. 125 (2019) 136–143.
[22] Y. Liang, C. Chen, Y. Zhao, B. Xia, W. Wu, J. Tang, Q. Chen, L. Tang, H. Yang, Z. Zhang, Y. Lu, Y. Yang, Neuroprotective effect of echinacoside in subacute mouse model of Parkinson's disease, BioMed Res. Int. 2019 (2019) 4379639.
[23] L. Li, Y. Wang, X. Qin, J. Zhang, Z. Zhang, Echinacoside protects retinal ganglion cells from ischemia/reperfusion-induced injury in the rat retina, Mol. Vis. 24 (2018) 746–758.
[24] E. Blasi, R. Barluzzi, V. Bocchini, R. Mazzolla, F. Bistoni, Immortalization of murine microglial cells by a v-raf/v-myc carrying retrovirus, J. Neuroimmunol. 27 (2–3) (1990) 229–237.
[25] D.M. Basso, M.S. Beattie, J.C. Bresnahan, A sensitive and reliable locomotor rating scale for open field testing in rats, J. Neurotrauma 12 (1) (1995) 1–21.
[26] E.C. Jensen, Quantitative analysis of histological staining and fluorescence using ImageJ, Anat. Rec. 296 (3) (2013) 378–381.
[27] Q. Zhao, X. Yang, D. Cai, L. Ye, Y. Hou, L. Zhang, J. Cheng, Y. Shen, K. Wang, Y. Bai, Echinacoside protects against MPP(+)-induced neuronal apoptosis via ROS/ATF3/CHOP pathway regulation, Neurosci. Bull. 32 (4) (2016) 349–362.
[28] A. Ulndreaj, J.C. Chio, C.S. Ahuja, M.G. Fehlings, Modulating the immune response in spinal cord injury, Expert Rev. Neurother. 16 (10) (2016) 1127–1129.
[29] Y.J. Shiao, M.H. Su, H.C. Lin, C.R. Wu, Echinacoside ameliorates the memory impairment and cholinergic deficit induced by amyloid beta peptides via the inhibition of amyloid deposition and toxicology, Food. Funct. 8 (6) (2017) 2283–2294.
[30] K. Mortezaee, N. Khanlarkhani, C. Beyer, A. Zendedel, Inflammasome: its role in traumatic brain and spinal cord injury, J. Cell. Physiol. 233 (7) (2018) 5160–5169.
[31] Y. Yang, H. Wang, M. Kouadir, H. Song, F. Shi, Recent advances in the mechanisms of NLRP3 inflammasome activation and its inhibitors, Cell Death Dis. 10 (2) (2019) 128.
[32] S. Voet, S. Srinivasan, M. Lamkanfi, Inflammasomes in neuroinflammatory and neurodegenerative diseases, EMBO Mol. Med. 11 (6) (2019) e10248.
[33] S. Vallabhapurapu, M. Karin, Regulation and function of NF-kappaB transcription factors in the immune system, Annu. Rev. Immunol. 27 (2009) 693–733.
[34] F.G. Bauernfeind, G. Horvath, A. Stutz, E.S. Alnemri, K. MacDonald, D. Speert, T. Fernandes-Alnemri, J. Wu, B.G. Monks, K.A. Fitzgerald, V. Hornung, E. Latz, Cutting edge: NF-kappaB activating pattern recognition and cytokine receptors license NLRP3 inflammasome activation by regulating NLRP3 expression, J. Immunol. 183 (2) (2009) 787–791.
[35] R. Kuang, Y. Sun, X. Zheng, Suppression of nitric oxide implicated in the protective effect of echinacoside on H2O2-induced PC12 cell injury, Nat. Prod. Commun. 5 (4) (2010) 571–574.
[36] J. Zhang, Z. Zhang, J. Xiang, M. Cai, Z. Yu, X. Li, T. Wu, D. Cai, Neuroprotective effects of echinacoside on regulating the stress-active p38MAPK and NF-kappaB p52 signals in the mice model of Parkinson's disease, Neurochem. Res. 42 (4) (2017) 975–985.
[37] K. Sas, E. Szabo, L. Vecsei, Mitochondria, oxidative stress and the kynurenine system, with a focus on ageing and neuroprotection, Molecules 23 (1) (2018).
[38] M.E. Heid, P.A. Keyel, C. Kamga, S. Shiva, S.C. Watkins, R.D. Salter, Mitochondrial reactive oxygen species induces NLRP3-dependent lysosomal damage and inflammasome activation, J. Immunol. 191 (10) (2013) 5230–5238.
[39] Q. Liu, D. Zhang, D. Hu, X. Zhou, Y. Zhou, The role of mitochondria in NLRP3 inflammasome activation, Mol. Immunol. 103 (2018) 115–124.
[40] R. Zhou, A.S. Yazdi, P. Menu, J. Tschopp, A role for mitochondria in NLRP3 inflammasome activation, Nature 469 (7329) (2011) 221–225.
[41] M.A. Anwar, T.S. Al Shehabi, A.H. Eid, Inflammogenesis of secondary spinal cord injury, Front. Cell. Neurosci. 10 (2016) 98.
[42] Y.H. Wang, Z.H. Xuan, S. Tian, G.H. Du, Echinacoside protects against 6-hydroxydopamine-induced mitochondrial dysfunction and inflammatory responses in PC12 cells via reducing ROS production, Evid-Based. Compl. Alt. (2015) 189239PMID: 25788961.
[43] H. Shi, Y. Wang, X. Li, X. Zhan, M. Tang, M. Fina, L. Su, D. Pratt, C.H. Bu, S. Hildebrand, S. Lyon, L. Scott, J. Quan, Q. Sun, J. Russell, S. Arnett, P. Jurek, D. Chen, V.V. Kravchenko, J.C. Mathison, E.M. Moresco, N.L. Monson, R.J. Ulevitch, B. Beutler, NLRP3 activation and mitosis are mutually exclusive events coordinated by NEK7, a new inflammasome component, Nat. Immunol. 17 (3) (2016) 250–258.
[44] Y. He, M.Y. Zeng, D. Yang, B. Motro, G. Nunez, NEK7 is an essential mediator of NLRP3 activation downstream of potassium efflux, Nature 530 (7590) (2016) 354–357.
[45] J.L. Schmid-Burgk, D. Chauhan, T. Schmidt, T.S. Ebert, J. Reinhardt, E. Endl, V. Hornung, A genome-wide CRISPR (clustered regularly interspaced short palindromic repeats) screen identifies NEK7 as an essential component of NLRP3 inflammasome activation, J. Biol. Chem. 291 (1) (2016) 103–109.
[46] A. Das, S.H. Kim, S. Arifuzzaman, T. Yoon, J.C. Chai, Y.S. Lee, K.S. Park, K.H. Jung, Y.G. Chai, Transcriptome sequencing reveals that LPS-triggered transcriptional responses in established microglia BV2 cell lines are poorly representative of primary microglia, J. Neuroinflammation 13 (1) (2016) 182.
[47] J. Jang, S. Park, H. Jin Hur, H.J. Cho, I. Hwang, Y. Pyo Kang, I. Im, H. Lee, E. Lee, W. Yang, H.C. Kang, S. Won Kwon, J.W. Yu, D.W. Kim, 25-hydroxycholesterol contributes to cerebral inflammation of X-linked adrenoleukodystrophy through activation of the NLRP3 inflammasome, Nat. Commun. 7 (2016) 13129.